

Synthesis, Characterization, and reactivity of Transition metal complexes with NHC ligands

M.Sc. Research Thesis

By

Sudhanshu Sekhar Majhi



**DEPARTMENT OF CHEMISTRY
INDIAN INSTITUTE OF TECHNOLOGY INDORE**

MAY 2024

**Synthesis, Characterization, and reactivity of Transition metal
complexes with NHC ligands**

A THESIS

*Submitted in partial fulfillment of the requirement
for the award of the degree*

of

Master of Science

by

Sudhanshu Sekhar Majhi

Roll no. 2203131017



**DEPARTMENT OF CHEMISTRY
INDIAN INSTITUTE OF TECHNOLOGY INDORE
MAY 2024**



INDIAN INSTITUTE OF TECHNOLOGY INDORE

CANDIDATE'S DECLARATION

I hereby certify that the work which is being presented in the thesis entitled “**Synthesis, Characterization and Reactivity of Transition Metal Complexes with NHC Ligands,**” in the partial fulfilment of the requirements for the award of the degree of **MASTER of SCIENCE** and submitted to the **DEPARTMENT of CHEMISTRY, Indian Institute of Technology Indore,** is an authentic record of my work carried out during the period July 2023 to May 2024 under the supervision of **Dr. Amrendra K. Singh,** Department of Chemistry, Indian Institute of Technology Indore. The matter presented in this thesis has not been submitted by me for the award of any other degree of this or any other institute.

Sudhanshu Sekhar Majhi
08/05/24

Sudhanshu Sekhar Majhi

Signature of the Student

This is to certify that the above statement made by the candidate is correct to the best of my/our knowledge.

Asingh.
8/5/2024

Dr. Amrendra K. Singh

Signature of the M.Sc. Thesis Supervisor

Sudhanshu Sekhar Majhi has successfully given his M. Sc. oral Examination held on 09/05/2024.

Asingh.

Signature of supervisor of M. Sc. Thesis

Date: 20/5/2024

Signature of Convener, DPGC

Date:

ACKNOWLEDGEMENTS

Initially, I express my gratitude towards my thesis supervisor, **Dr. Amrendra Kumar Singh**, for providing me with valuable guidance, suggestions, and supervision, as well as for offering constant encouragement throughout my research work. Additionally, I express my gratitude to the members of my PSpC, **Prof. Suman Mukhopadhyay** and **Prof. Chelvam Venkatesh**, for their significant contributions and assistance. I am thankful to the **Department of Chemistry** at IIT Indore for providing me with the opportunity to undertake this research endeavor. Special acknowledgment goes to **Prof. Tushar Kanti Mukherjee**, the Head of the Department of Chemistry at the Indian Institute of Technology Indore, for his support and encouragement. I feel incredibly obligated to take this chance to express my gratitude to the teachers and SIC personnel at IIT Indore for their support and cooperation throughout this dissertation project.

I would like to extend my gratitude to my laboratory colleagues **Mr. Shambhu Nath Gupta, Mr. Navdeep Srivastava, Ms. Ekta Yadav, Ms. Achena Saha, Ms. Nida Shahid, Mr. Ashu Singh, Mr. Rahul Kumar Singh, Mr. Vishal Jaiswal, and Mr. Naveen Kumar** who consistently provided me with valuable insights and unwavering support in pursuit of the project's objectives. The information that you generously imparted to me was greatly motivating, not only for the present undertaking but also for the broader realm of communication practice. I want to express my gratitude to my brothers, who have always supported me and never let me down throughout my life. Finally, I'd like to express my deepest appreciation to my parents for all their support and encouragement during the duration of this endeavour.

Sudhanshu Sekhar Majhi

M. Sc. 2nd year

Roll No. 2203131017

Department of Chemistry

*Dedicated to
my Parents*

ABSTRACT

Water oxidation catalysis has emerged as a pivotal research area in the quest for sustainable energy conversion technologies. Various methodologies using Ruthenium-based catalysts have been reported in the field of water oxidation catalysis. In this report, we present our work on the synthesis and characterization of pincer ligand-based ruthenium complexes which is analogous to the previously reported terpyridine and bipyridyl-based water oxidation catalyst. The Ru (II) CNC aqua complex has been characterized by ^1H NMR, ^{13}C NMR, ^{31}P NMR, and mass spectrometry. The catalytic activity of CNC-based metal complexes toward water oxidation catalysts has been explored.

TABLE OF CONTENTS

LIST OF FIGURES	IX
LIST OF SCHEMES	X
ACRONYMS	XI
NOMENCLATURE	XII
CHAPTER 1: INTRODUCTION	1-5
1.1 Aim of the experiment	1
1.2 General Introduction	1-2
1.3 N-Heterocyclic carbene	2-3
1.4 Water oxidation catalysis	3-5
CHAPTER 2: EXPERIMENTAL SECTION	6-10
2.1 General information	6
2.2 Chemicals and reagents	6
2.3. Instrumentation	6
2.4.1 Synthesis of Ligand L1	6-7
2.4.2 Synthesis of Ligand L2	7
2.4.3 Synthesis of Ligand L3	7-8
2.4.4 Synthesis of Ligand L4	8
2.4.5 Synthesis of Ligand L5	8
2.5.1 Synthesis of Precursor P1	9
2.5.2 Synthesis of precursor P2	9
2.5.3 Syntesis of Precursor P3	9
2.5.4 Synthesis of Complex Ru1	9-10
2.5.5 Synthesis of Complex Ru2	10
CHAPTER 3: RESULTS AND DISCUSSION	11-31
3.11 Characterization of Ligand L1	15-16
3.12 Characterization of Ligand L2	16-17
3.13 Characterization of Ligand L3	18-19
3.14 Characterization of Ligand L4	19-20
3.15 Characterization of Ligand L5	20-21
3.16 Characterization of Complex Ru1	21-24

3.17 Characterization of Complex Ru ₂	25-26
3.18 Catalytic applications	26-31
CHAPTER 4: CONCLUSION	32
References	33-36

LIST OF FIGURES

Fig.1: N-Heterocyclic carbenes

Fig.2: First stable N-Heterocyclic carbene.

Fig.3: Previously reported catalysts.

Fig.4: LCMS of Ligand L1

Fig.5: ^1H NMR of Ligand L1

Fig.6: ^{13}C NMR of Ligand L1

Fig.7: LCMS of Ligand L2

Fig.8: ^1H NMR of Ligand L2

Fig.9: ^{13}C NMR of Ligand L2

Fig.10: LCMS of Ligand L3

Fig.11: ^1H NMR of Ligand L3

Fig.12: ^{13}C NMR of Ligand L3

Fig.13: ^1H NMR of Ligand L4

Fig.14: ^{13}C NMR of Ligand L4

Fig.15: ^1H NMR of Ligand L5

Fig.16: ^{13}C NMR of Ligand L5

Fig.17: HRMS of Complex Ru1

Fig.18: ^1H NMR of Complex Ru1

Fig.19: ^{13}C NMR of Complex Ru1

Fig.20: ^{31}P NMR of Complex Ru1

Fig.21: ^1H NMR of complex Ru1

Fig.22: ^{13}C NMR of Complex Ru1

Fig.23: ^{31}P NMR of complex Ru1

Fig.24: LCMS of Complex Ru2

List of Schemes

Scheme 1. Synthesis of ligand **L1**

Scheme 2. Synthesis of ligand **L2**

Scheme 3. Synthesis of ligand **L3**

Scheme 4. Synthesis of ligand **L4**

Scheme 5. Synthesis of ligand **L5**

Scheme 6. Synthesis of precursor **P1**

Scheme 7. Synthesis of precursor **P2**

Scheme 8. Synthesis of precursor **P3**

Scheme 9. Synthesis of Complex **Ru1**

Scheme 10. Synthesis of Complex **Ru2**

Scheme 11. Oxygen evolution experiment in 0.1 M HNO₃

Scheme 12. Oxygen evolution experiment in 0.1 CF₃SO₃H

Scheme 13. Oxygen evolution experiment in 0.1 M HClO₄

Scheme 14. Oxygen evolution experiment in 0.1 M HNO₃

Scheme 15. Oxygen evolution experiment in 0.1 M HNO₃

Scheme 16. Oxygen evolution experiment in 0.1 M HNO₃

Scheme 17. Oxygen evolution experiment in 0.1 M HNO₃

Scheme 18. Oxygen evolution experiment in 0.1 M HClO₄

Scheme 19. Oxygen evolution experiment in 0.1 M HClO₄

ACRONYMS

ACN	Acetonitrile
CAN	Ceric ammonium nitrate
CDCl ₃	Chloroform-d
CHCl ₃	Chloroform
DCM	Dichloromethane
DMSO	Dimethyl sulfoxide
ESI	Electron spray ionization
HRMS	High-resolution mass spectrometry
K ₂ CO ₃	Potassium carbonate
LCMS	Liquid chromatography-mass spectrometry
MeOH	Methanol
Na ₂ SO ₄	Sodium sulfate
NMR	Nuclear magnetic resonance
NH ₄ Cl	Ammonium chloride
TLC	Thin layer chromatography

NOMENCLATURE

°C	Degree Celsius
h	hour
Hz	Hertz
M	Molar
mL	Millilitre
mg	Milligrams
MHz	megahertz
mmol	millimole
nm	Nanometer
ppm	Parts per million

CHAPTER 1

INTRODUCTION

1.1 Aim of the project:

In our laboratory, we have achieved significant milestones in the synthesis of various iodobased CNC ruthenium pincer complexes. [1-2] Expanding our groundwork we have recently synthesized novels CNC-based Ru (II) aqua complex drawing parallels to the previously reported ruthenium terpyridine and bipyramidal framework. [3-4] We are excited about the potential of this complex as a high-performance water oxidation catalyst. We look forward to further exploring its capabilities and advancing our understanding in this field.

1.2 General Introduction:

The use of ruthenium pincer complexes as catalysts has gained significant attention in recent years due to their ability to control reactivity, stability, and selectivity in various chemical reactions and catalyst designs.[5] The tridentate pincer ligands, particularly those incorporating N-Heterocyclic carbene (NHCs) are highly versatile in organometallic chemistry and catalysis due to their exceptional stereo electronic diversity and ability to form stable compounds.[6] The pyridine dicarbene pincer ligands, which contain N-heterocyclic carbene are particularly popular due to their ability to increase the electron density at the Ruthenium Centre, thereby enhancing its reactivity. [7] N-heterocyclic carbene has indeed gained significant popularity as a transition metal ligand in these years in recent years due to its unique properties and versatility. The unique properties and wide-ranging applications make them an exciting area of research with great potential for future developments. This increased reactivity makes ruthenium complexes attractive for a wide range of catalytic applications.[8] In summary, Ruthenium complexes are highly versatile coordination compounds that find applications across diverse fields including photochemistry, photophysics, bioinorganic chemistry, and catalysis. From a catalytic point of view, ruthenium complexes have demonstrated

in a significant number of reactions including C-H activation, C-C coupling, C-H insertion, and Redox Catalysis with organic transformations. the catalytic reactions have proven to be valuable in organic synthesis and industrial processes.^[9]

1.3 N-Heterocyclic carbene (NHC):

N-heterocyclic carbenes (NHC) are a class of organic compounds that contain a neutral two-electron donor ligand featuring a nitrogen atom in a heterocyclic ring. NHCs are known for their strong electron-donating properties and stability compared to traditional carbenes. The appeal of NHC ligands lies in their highly modular molecular structure, distinctive electronic and steric characteristics, and ability to form robust NHC-metal bonds. These properties make them versatile and flexible for various applications in organometallic chemistry, catalysis, and materials science.^[10] The stability of NHC-metal complexes offers efficient and selective reactions in catalysis. They can form stable complexes with a wide range of metals leading to enhanced reactivity and selectivity in various transformations. The field of NHC chemistry indeed originated in 1968 with the pioneering work of Ofele ^[11] and Wanzlick ^[12] which initially focused on metal coordination compounds derived from azolium precursors. However, in 1991, the field experienced a notable resurgence following the groundbreaking demonstration of free carbenes accessibility by Arduengo.^[13] The N-Heterocyclic carbene spread in diverse catalytic processes including Heck, Sonogashira, and Suzuki Cross-coupling reactions, Hydrogenation, C-H activation, and olefin metathesis. The stability of NHC-based transition metal complexes allows for efficient catalyst utilization leading to the development of novel synthetic methodologies and synthesis of complex organic molecules.^[14] The development has revitalized interest in NHC chemistry particularly due to the potential of heterocyclic carbene ligands in organometallic catalysts representing a key motivation for renowned attention to this area of study.

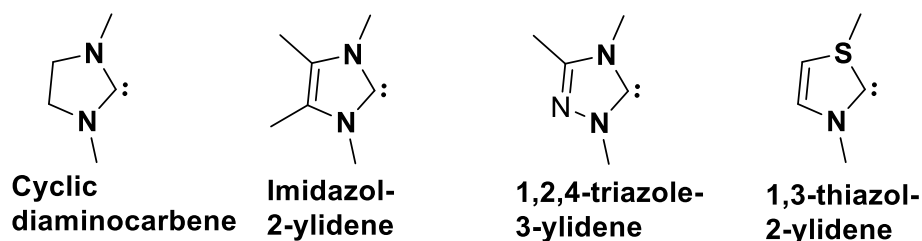


Fig.1: N-Heterocyclic carbenes

1. The NHC differs from the most electron-rich for phosphine in terms of its σ -donation and by π -acceptance properties.
2. NHC Ligands are easily modifiable to fine-tune their steric and electronic properties by controlling their reactivity and selectivity of metal-catalyzed reactions.
3. The high thermal stability of metal NHC complexes along with the ability to adjust their steady and electronic properties make them appealing characteristics for advancing Organometallic materials.

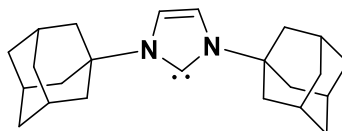


Fig.2: First stable N-Heterocyclic carbene.^[15]

1.4 Water Oxidation Catalysis:

Water oxidation plays a crucial role in energy storage, especially in the context of renewable energy sources, as we strive towards sustainable energy, efficient energy storage, and hydrogen production are of utmost importance.^[16] Our promising method to achieve energy storage via water splitting involves oxidizing water to generate oxygen. Therefore, developing an efficient water oxidation catalyst is critical to the success of this approach. Various metal-based catalysts including Ruthenium, Iridium, and Cobalt have been explored for their potential as water Oxidation catalysts.^[17-19] Efficient water oxidation catalysts are essential for the development of high-performance energy storage systems based

on water splitting. The hydrogen fuel produced through this process can be utilised in fuel cells to generate electrical energy providing a clean and sustainable alternative to traditional fuel fuels. Furthermore, the oxygen generated during water oxidation can be used in various industrial processes such as the production of chemicals and fuels.^[20] Overall, water oxidation represents a crucial step in the development of sustainable energy storage systems, and continuous research into efficient water oxidation catalysts is necessary to fully realize the potential of this approach.

Inspired by the natural photosynthesis process several researchers have been working on developing artificial systems that can mimic the natural photosynthesis process and split water into oxygen and Hydrogen.^[21] In 1982 a team of researchers super headed by Meyer Made a revolutionary breakthrough known as the “Blue dimer”.^[22] This dinuclear ruthenium complex $[(bpy)_2(OH_2) RuORu (OH_2) (bpy)_2]^{4+}$ was unprecedented in its ability to perform a significant electrocatalytic process which involved oxidizing water and generating dioxygen. This discovery marked a significant milestone in the field of electrochemistry, paving the way for new possibilities and opportunities for further research in this area.

Thummel et al. in 2005 made a significant breakthrough by creating the First ever mononuclear nuclear Ruthenium water oxidation catalyst.^[23] The catalyst has found widespread use in sustainable energy applications, specifically in converting solar energy to chemical energy through the process of water molecule splitting, resulting in the production of oxygen and hydrogen. The development of these catalysts has opened up new avenues for researchers to explore more efficient and cost-effective ways to produce clean energy. In 2019, Ahlquist and colleagues provided valuable evidence to support the involvement of a dangling carboxylate group in facilitating proton-coupled electron transfer (PCET) reactions. This was achieved through the use of an intramolecular proton relay, which allowed for a better understanding of the underlying mechanisms involved.^[24]

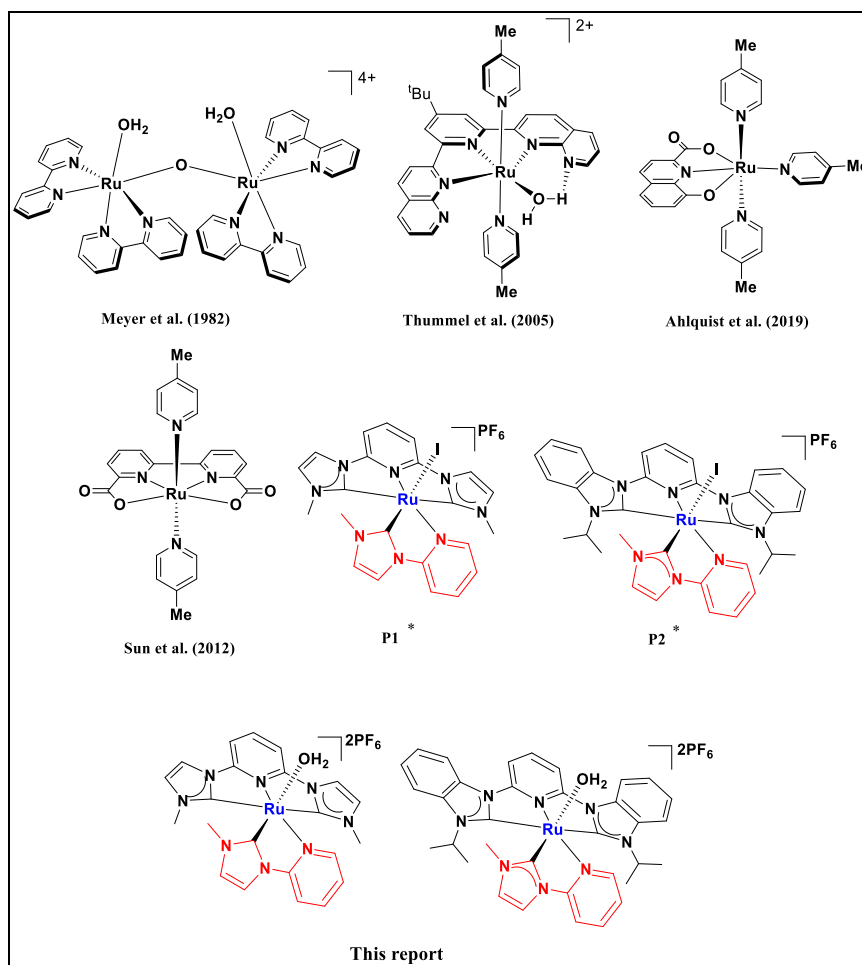


Fig.3: Previously reported water oxidation catalysts. (*These complexes were synthesized in our lab)

In 2012, Son and his research group have made a significant breakthrough by recently developing a highly water oxidation catalyst [Ru(bda)(pic)₂].^[25] This catalyst has the potential to revolutionize the field of water oxidation by making it easier and more efficient to generate oxygen from water. In the scientific community, the Ru-bda core has gained wide recognition and popularity as a valuable building block for constructing various molecular devices and Supramolecular systems. Its versatility and stability make it an ideal candidate for developing new technologies in fields such as catalysis photochemistry and molecular electronics.

CHAPTER-2

EXPERIMENTAL SECTION

2.1 General information:

All of the chemicals and solvents used in this study were purchased from commercially accessible sources. No purification was done before their use. However, hexane and ethyl acetate were distilled before usage. The experiments were conducted in a nitrogen-filled Schlenk line. The results were monitored using Merck 60 F254 precoated silica gel plates for thin-layer chromatography (TLC). To purify the products, column chromatography with silica gel (100-200 mesh) was employed.

2.2 Chemicals and Reagents:

Without any additional purification, all of the reagents and solvents utilized in this experiment were obtained from commercial sources.

These chemicals include Benzimidazole (SRL, 99%), imidazole (SRL, 99%), 2,6- dibromo pyridine (Alfa Aesar, 98%), 2-bromo pyridine (Spectrochem, 99%), potassium carbonate (SRL, 99.5%), sodium bicarbonate (SRL, 99.5%), ruthenium trichloride trihydrate (SRL), potassium hydroxide (Emplura, 85%), Sodium hydroxide (Emplura, 84%), Methyl iodide (Spectrochem, 99%), Isopropyl bromide (Spectrochem, 99%), 1-Methylimidazole (Spectrochem, 99%).

2.3 Instrumentation:

The ADVANCE III 400 and 500MHz Ascend Bruker BioSpin machines were used to record NMR spectra at ambient temperature. For mass spectrometric analyses, the Bruker-Daltonics micro to-Q II mass spectrometer was utilized.

2.4 SYNTHESIS OF LIGANDS:

2.4.1 Synthesis of Ligand L1:

Experimental procedure:

NaOH (2.03g, 50.78 mol) and benzimidazole (4g, 33.85 mol) were added to an oven-dried two-neck round-bottom flask and dissolved in

30 mL of DMSO. After agitating the solution at room temperature for a full twelve hours, 4.76 mL of isopropyl bromide was added, and the reaction mixture was left to agitate. Following completion, the reaction solvent was removed using cold water and DCM, and it was then dried over sodium sulfate. The rotatory evaporator was then used to evaporate the solvent and produce the necessary pale yellow liquid. Yield: 3.50g, 65% and the characterization for ^1H NMR and ^{13}C NMR data, which shows the confirmation of the ligand. ^1H NMR (500 MHz, CDCl_3) δ 7.94 (s, 1H), 7.81 – 7.76 (m, 1H), 7.40 – 7.34 (m, 1H), 7.26 – 7.20 (m, 2H), 4.55 (hept, $J = 6.7$ Hz, 1H), 1.54 (d, $J = 7.1$ Hz, 6H). $^{13}\text{C}\{^1\text{H}\}$ NMR (126 MHz, CDCl_3) δ 143.95, 140.11, 133.15, 122.48, 121.88, 120.26, 110.02, 47.53, 22.43.

2.4.2 Synthesis of Ligand L2:

2-bromopyridine (1.81 mL, 18.98 mol), imidazole (1.55 g, 22.77 mol), KOH (1.64 g, 28.47 mol), and CuI (0.54 g, 2.84 mol) were charged into a two-neck round-bottom flask that had been oven-dried and dissolved in 30 mL of DMSO solvent. For 24 hours, the reaction mixture was refluxed at 120 °C. Following completion, the reaction mixture was vacuum-filtered through cold water and Celite, and the solvent DMSO was extracted using DCM. The solvent was then evaporated by the rotatory evaporator to afford a pale-yellow liquid product. Yield: 2.10g, 76%, and the characterization for ^1H NMR and ^{13}C NMR data, which show the pure ligand, were obtained thereafter. ^1H NMR (500 MHz, CDCl_3) δ 8.62 (s, 1H), 8.52 (s, 1H), 8.01 – 7.90 (m, 1H), 7.80 (s, 1H), 7.51 (d, $J = 7.5$ Hz, 1H), 7.44 – 7.36 (m, 1H), 7.35 (s, 1H). $^{13}\text{C}\{^1\text{H}\}$ NMR (126 MHz, CDCl_3) δ 149.26, 139.22, 135.49, 135.09, 130.68, 122.23, 116.35, 112.50.

2.4.3 Synthesis of Ligand L3:

After adding 25 mL of EtOAc to a Schlenk tube containing 2.5 g of pyridyl imidazole (17.24 mol) and 1.60 ml of methyl iodide (25.86 mol), the reaction mixture was refluxed for 12 hours under a nitrogen

environment. Following completion, diethyl ether was used to wash the mixture, yielding a white precipitated product. Yield: 3.55g, 71.8%. The product was confirmed by ^1H NMR and ^{13}C NMR spectroscopy. ^1H NMR (500 MHz, CDCl_3) δ 11.00 (s, 1H), 8.51 (dd, $J = 4.9, 1.8$ Hz, 1H), 8.33 (d, $J = 8.3$ Hz, 1H), 8.27 (d, $J = 2.1$ Hz, 1H), 8.02 (td, $J = 7.9, 1.9$ Hz, 1H), 7.71 (d, $J = 2.0$ Hz, 1H), 7.46 (dd, $J = 7.6, 4.8$ Hz, 1H), 4.30 (s, 3H). $^{13}\text{C}\{^1\text{H}\}$ NMR (126 MHz, CDCl_3) δ 149.04, 145.65, 140.41, 135.00, 125.14, 124.13, 118.79, 114.69, 37.59.

2.4.4 Synthesis of Ligand L4:

Ligand L1 (3.50 mL, 21.87 mmol) was added to 2,6-dibromo pyridine (2.254 g, 9.51 mmol) in a thick walled pressure tube. For five days, the well-mixed reaction mixture was heated to 150 °C and stirred. The solid residue that was left behind after the reaction was cooled to room temperature was dissolved in MeOH, diethyl ether was added, and the white precipitate triazolium salt emerged. ^1H NMR (500 MHz, $\text{DMSO-}d_6$) δ 10.68 (s, 2H), 8.78 (t, $J = 8.1$ Hz, 1H), 8.45 (dd, $J = 11.9, 8.3$ Hz, 4H), 8.32 (d, $J = 8.4$ Hz, 2H), 7.80 (ddd, $J = 8.3, 7.2, 1.1$ Hz, 2H), 7.71 (ddd, $J = 8.4, 7.2, 1.0$ Hz, 2H), 5.27 (hept, $J = 6.7$ Hz, 2H), 1.78 (d, $J = 6.7$ Hz, 12H). $^{13}\text{C}\{^1\text{H}\}$ NMR (126 MHz, $\text{DMSO-}d_6$) δ 146.44, 144.18, 141.53, 131.03, 129.78, 127.87, 127.33, 118.26, 115.84, 114.54, 54.93, 39.52, 21.55.

2.4.5 Synthesis of Ligand L5:

1-methyl imidazole (2.018 mL, 25.328 mol) was combined with 1.50 g, 6.332 mol of 2,6-dibromo pyridine in a pressure tube with thick walls. For three days, the clean reaction mixture was heated to 150 °C while being agitated. The solid residue that was left over after the reaction was cooled to room temperature was dissolved in MeOH, and when diethyl ether was added, a brown precipitate of triazolium salt emerged.

^1H NMR (500 MHz, $\text{DMSO-}d_6$) δ 10.12 (s, 2H), 8.50 (s, 2H), 8.39 (t, $J = 8.1$ Hz, 1H), 8.04 (d, $J = 8.1$ Hz, 2H), 7.80 (s, 2H), 3.96 (s, 7H). $^{13}\text{C}\{^1\text{H}\}$ NMR (126 MHz, $\text{DMSO-}d_6$) δ 145.97, 145.69, 136.53, 125.72, 119.92, 115.02, 37.35.

2.5 SYNTHESIS OF COMPLEXES:

2.5.1 Synthesis of Precursor P1:

In a Schlenk tube imidazolium salt **L3** (329.56 mg, 1.147 mmol), Ruthenium precursor (300 mg, 1.147) and THF solvent were added to it. The reaction mixture was refluxed at 60 °C for 12h. After completion, the reaction mixture was filtered and washed through THF, resulting brown precipitate was obtained.

2.5.2 Synthesis of precursor P2:

Taking the pincer ligand precursor **L4** (500 mg, 1.258 mmol) and ruthenium precursor **P1** (485.54 mg, 1.258 mmol) in a Schlenk tube. The mixture was then refluxed at 190 °C in ethylene glycol conditions. Subsequently, saturated solutions of KPF_6 were added to the mixture. After the completion of the reaction, the mixture was allowed to cool, washed with diethyl ether, and filtered to obtain a dark yellow solid precipitate.

2.5.3 Synthesis of precursor P3:

In the Schlenk tube, we took 187.7 mg (0.466 mmol) of pincer ligand precursor **L5** and 180 mg (0.466 mmol) of ruthenium precursor **P1**, which were then refluxed 190 °C in ethylene glycol conditions. Next, we added saturated solutions of KPF_6 and allowed the reaction to complete. The resulting mixture was washed with diethyl ether and filtered to obtain a dark brown solid precipitate.

2.5.4 Synthesis of complex Ru1:

In a clean and dry Schlenk, both precursor complex **P2** (100 mg, 0.107 mmol) and AgPF_6 (27.24 mg, 0.107 mmol) were taken. Water and THF were added to the tube in a ratio of 1:3, and the reaction mixture was stirred at room temperature for three hours. After completion of the reaction, the mixture was cooled down and washed with acetone. The mixture was then filtered through celite to obtain a solid which was washed with diethyl ether to obtain a precipitate. Yield: 43mg, 41.74 %.

The ligand is characterized through ^1H NMR, ^{13}C NMR, and ^{31}P NMR spectroscopy. ^1H NMR (500 MHz, $\text{DMSO-}d_6$) δ 9.74 (d, $J = 5.8$ Hz, 1H), 8.65 – 8.53 (m, 4H), 8.48 (d, $J = 22.7$ Hz, 4H), 7.96 (d, $J = 8.2$ Hz, 2H), 7.84 (s, 1H), 7.60 (t, $J = 7.9$ Hz, 2H), 7.52 (t, $J = 7.8$ Hz, 2H), 7.34 (s, 1H), 3.83 (p, $J = 7.2$ Hz, 2H), 2.53 (s, 3H), 1.53 (d, $J = 7.0$ Hz, 7H), 0.91 (d, $J = 7.2$ Hz, 7H). $^{13}\text{C}\{^1\text{H}\}$ NMR (126 MHz, $\text{DMSO-}d_6$) δ 197.02, 181.76, 153.75, 152.57, 132.87, 132.57, 124.79, 124.73, 123.65, 115.99, 113.57, 113.54, 112.94, 109.25, 53.31, 34.69, 20.15, 19.53. $^{31}\text{P}\{^1\text{H}\}$ NMR (202 MHz, $\text{DMSO-}d_6$) δ -15.05, -137.16, -140.67, -144.19, -147.70, -151.21.

2.5.5 Synthesis of complex Ru2:

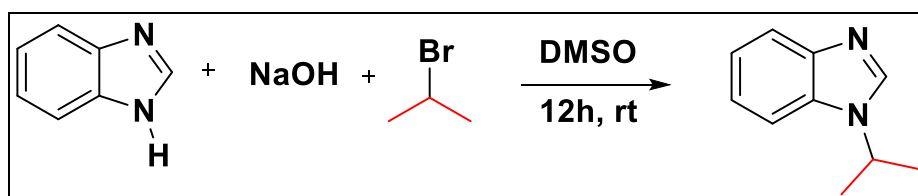
In a clean and dry Schlenk, both the metal precursor complex **P3** (100 mg, 0.129 mmol) and AgPF_6 (26.20 mg, 0.129 mmol) were taken. Water and THF were added to the tube in a ratio of 1:3, and the reaction mixture was stirred at room temperature for three hours. After completion of the reaction, the mixture was cooled down and washed with acetone. The mixture was then filtered through celite to obtain a solid which was washed with diethyl ether to obtain a precipitate. Yield: 38mg, 36.53%. The complex was characterized through ^1H NMR, ^{13}C NMR, and ^{31}P NMR spectroscopy. ^1H NMR (500 MHz, $\text{DMSO-}d_6$) δ 9.81 (d, $J = 5.8$ Hz, 1H), 8.50 (d, $J = 2.2$ Hz, 2H), 8.44 – 8.40 (m, 2H), 8.29 – 8.27 (m, 2H), 8.10 (d, $J = 8.3$ Hz, 2H), 7.65 (td, $J = 5.6, 4.0$ Hz, 1H), 7.57 (d, $J = 2.2$ Hz, 2H), 7.30 (d, $J = 2.2$ Hz, 1H), 3.12 (s, 6H), 2.54 (s, 3H). $^{13}\text{C}\{^1\text{H}\}$ NMR (126 MHz, $\text{DMSO-}d_6$) δ 187.24, 183.53, 153.58, 152.69, 152.33, 141.75, 139.20, 126.17, 125.57, 122.68, 118.83, 116.57, 112.89, 108.10, 36.00, 34.33. $^{31}\text{P}\{^1\text{H}\}$ NMR (202 MHz, $\text{DMSO-}d_6$) δ -133.65, -137.16, -140.68, -144.19, -147.71, -151.21, -154.73.

CHAPTER 3

RESULT AND DISCUSSION

3.1 Synthesis of Ligand L1:

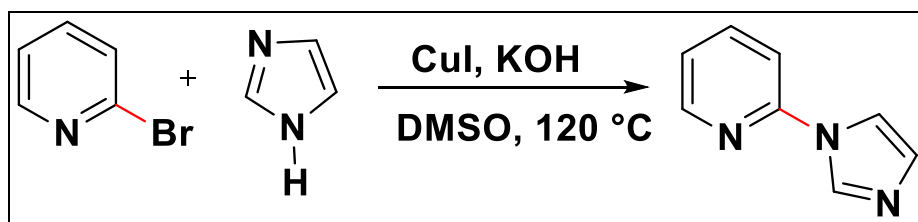
The ligand (L1) was synthesized by dissolving NaOH in DMSO and stirring at room temperature for two hours. After that, isopropyl bromide was added to the mixture and continually agitated until the mixture solidified into wax. The ^1H NMR data claimed the existence of this compound by giving the resonance δ 1.51 (s) for six protons of two methyl groups and δ 4.56 (hept) for the tertiary proton. The other 4 protons come in the aromatic region. (Scheme 1)



Scheme 1: Synthesis of Ligand L1

3.2 Synthesis of Ligand L2:

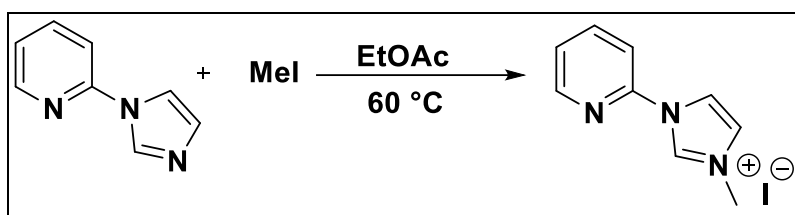
Ligand L2 was synthesized via the reported procedure by subjecting 2-bromopyridine, imidazole, to a reaction in dry DMSO in the presence of KOH as a base and CuI as a catalyst, as depicted in Scheme 2. ^1H and ^{13}C NMR were used to characterize the pale-yellow liquid that was obtained. The existence of this ligand is claimed by ^1H NMR by giving resonance at δ 8.62 (s) for carbenic protons and the rest protons are in the aromatic region.



Scheme 2: Synthesis of Ligand L2

3.3 Synthesis of Ligand **L3**:

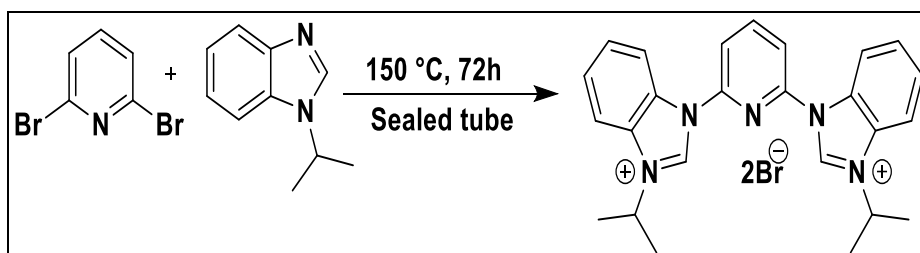
As depicted in **Scheme 3**, the methylation of ligand **L3** was carried out using methyl iodide, resulting in a final whitish solid product, ^1H NMR which confirmed the existence of this compound by giving the resonance at δ 11.00(s) for the carbenic proton flanked by two nitrogen atoms and δ 3.32 for the methyl group.



Scheme 3: Synthesis of Ligand **L3**

3.4 Synthesis of Ligand **L4**:

We have synthesized ligand **L4** by treating benzimidazole and 2,6-dibromo pyridine at 150 °C for 4 hours. A solid form of the final chemical was produced. ^1H and ^{13}C NMR spectroscopy were used to characterize the product. The ^1H NMR data claimed the existence of this compound by giving the resonance δ 10.68 (s) for the carbenic proton and δ 1.78(d) for twelve methyl protons.

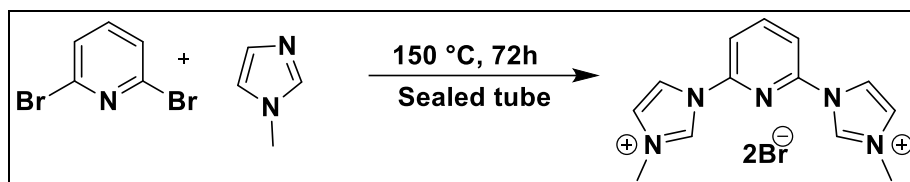


Scheme 4: Synthesis of Ligand **L4**

3.5 Synthesis of Ligand **L5**:

We have synthesized ligand **L5** by treating imidazole and 2,6-dibromo pyridine at 150 °C for 4 hours. A solid form of the final chemical was developed. Through the use of ^1H and ^{13}C NMR spectroscopy, the

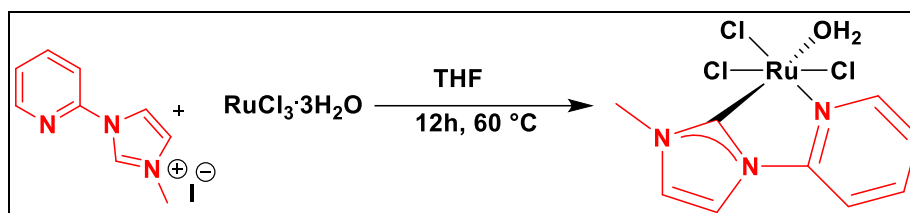
product was described. ^1H NMR data claimed the existence of this compound by giving the resonance δ 10.12 (s) for the carbenic proton and δ 3.46(s) for two methyl protons. The rest protons come in aromatic region.



Scheme 5: Synthesis of Ligand **L5**

3.6 Synthesis of Precursor **P1**:

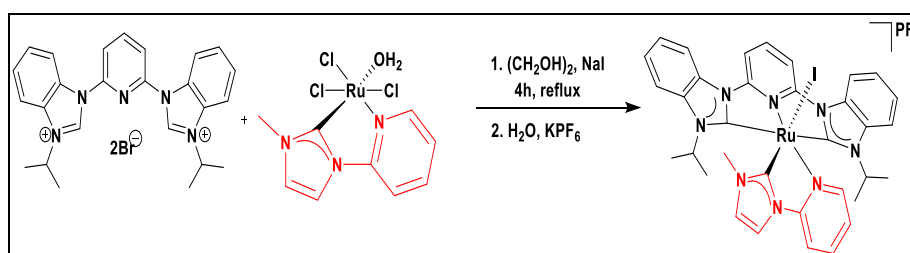
Metal precursor complex **P1** was synthesized by reacting Ligand **L3** with ruthenium trichloride trihydrate ($\text{RuCl}_3 \cdot 3\text{H}_2\text{O}$) in THF solvent at a temperature of $65\text{ }^\circ\text{C}$ for 12 hours, as shown in Scheme 5. The precursor (**P1**) was obtained with a yield of 60.76%. Subsequently, Metal precursor complex **P1** was characterized using UV spectrometry.



Scheme 6: Synthesis of precursor **P1**

3.7 Synthesis of precursor **P2**:

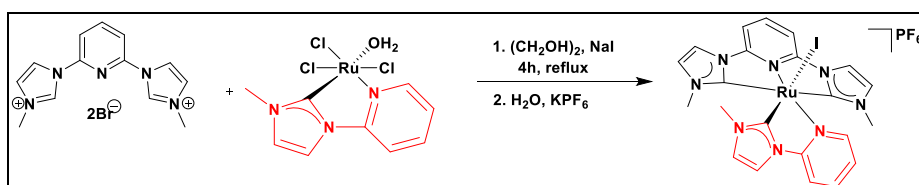
To synthesize the complex, the ligand **L4** and ruthenium precursor **P1** is dissolved in ethylene glycol and refluxed under Nitrogen for 4 hours followed by saturated solutions of KPF_6 was added. The synthesized complex was confirmed by ^1H NMR, ^{13}C NMR, and ^{31}P NMR spectroscopy.



Scheme 7: Synthesis of precursor **P2**

3.8 Synthesis of precursor P3:

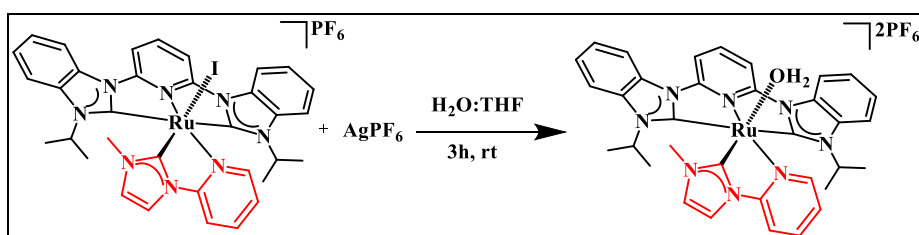
To synthesize the complex, the ligand **L5** and ruthenium precursor **P1** is dissolved in ethylene glycol and refluxed under Nitrogen for 4 hours followed by saturated solutions of KPF_6 was added. The synthesized complex was confirmed by ^1H NMR, ^{13}C NMR, and ^{31}P NMR spectroscopy.



Scheme 8: Synthesis of precursor **P3**

3.9 Synthesis of complex Ru1:

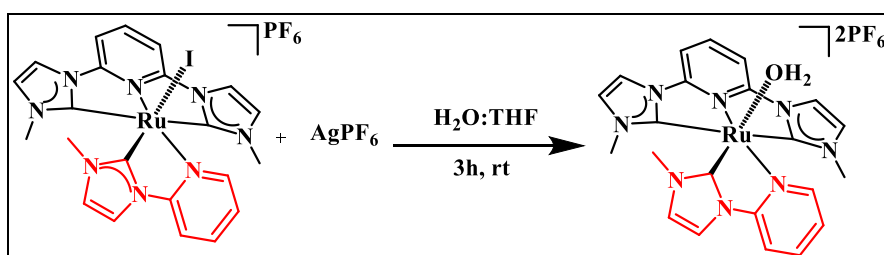
The metal precursor **P2** and AgPF_6 were combined in a 1:3 ratio with H_2O : THF and agitated for three hours at room temperature in order to create complex **Ru1**. Using ^1H , ^{13}C , and ^{31}P NMR spectroscopy, the produced compound was verified.



Scheme 9: Synthesis of complex **Ru1**

3.10 Synthesis of complex Ru2:

The metal precursor **P3** and AgPF_6 were combined in a 1:3 ratio with H_2O : THF and agitated for three hours at room temperature to synthesize the complex **Ru2**. Using ^1H , ^{13}C , and ^{31}P NMR spectroscopy, the produced compound was confirmed.



Scheme 10: Synthesis of complex **Ru2**

3.11 Characterization of Ligand L1

3.11.1 LCMS of Ligand L1

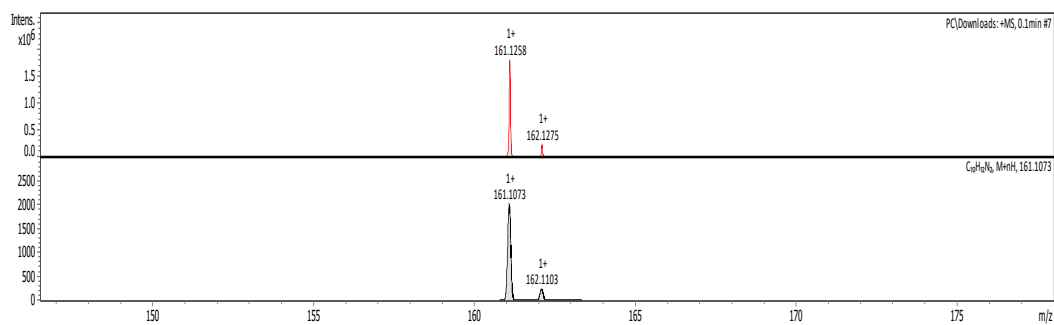


Fig.4: LCMS of Ligand L1

3.11.2 NMR spectra of Ligand L1

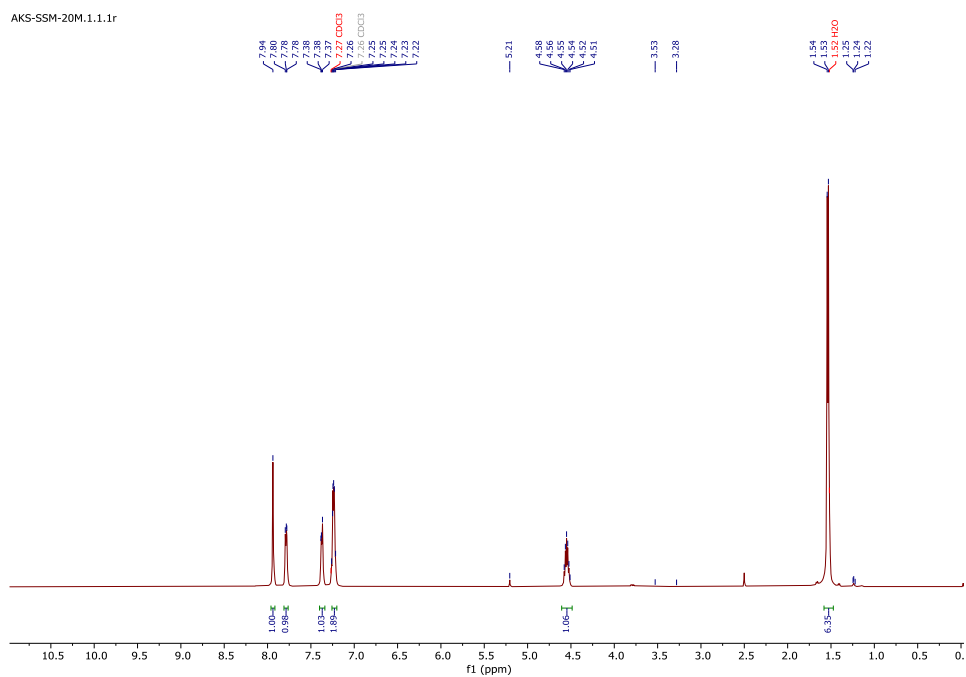


Fig.5: ¹H NMR of Ligand L1

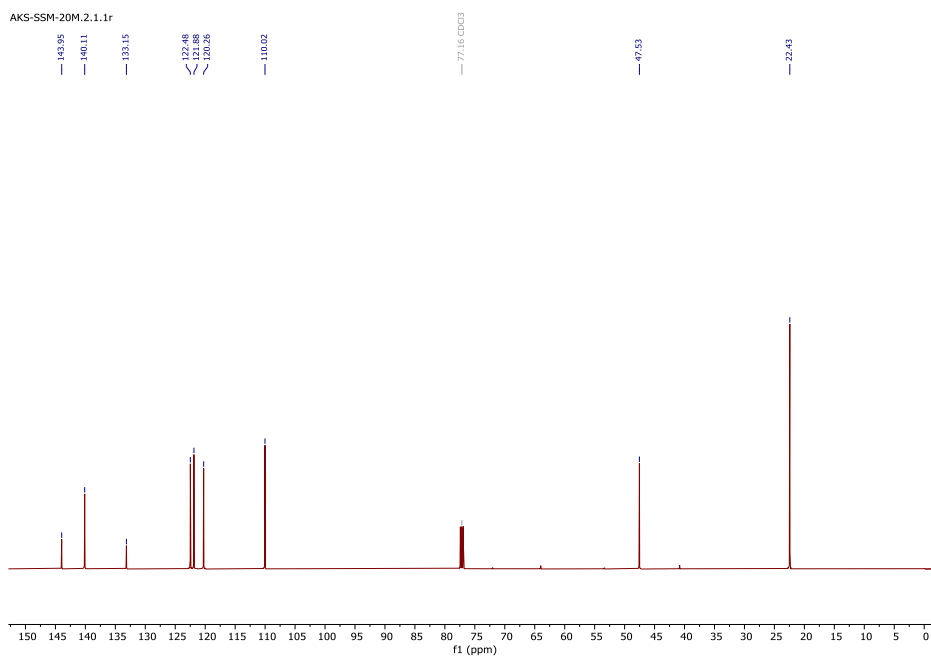


Fig.6: ¹³C NMR of Ligand L1

3.12 Characterization of Ligand L2

3.12.1 LCMS of Ligand L2

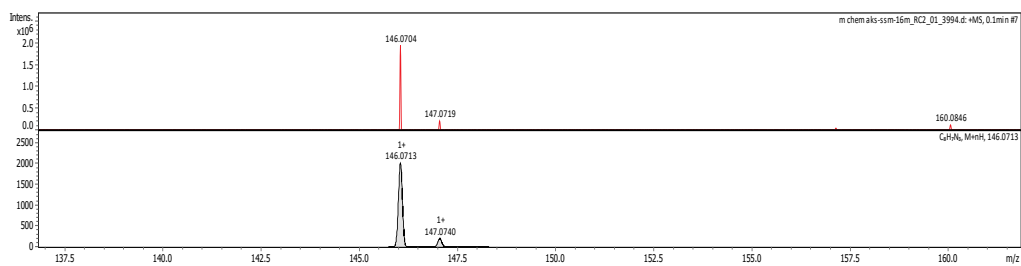


Fig.7: LCMS of Ligand L2

3.12.2 NMR spectra of Ligand L2

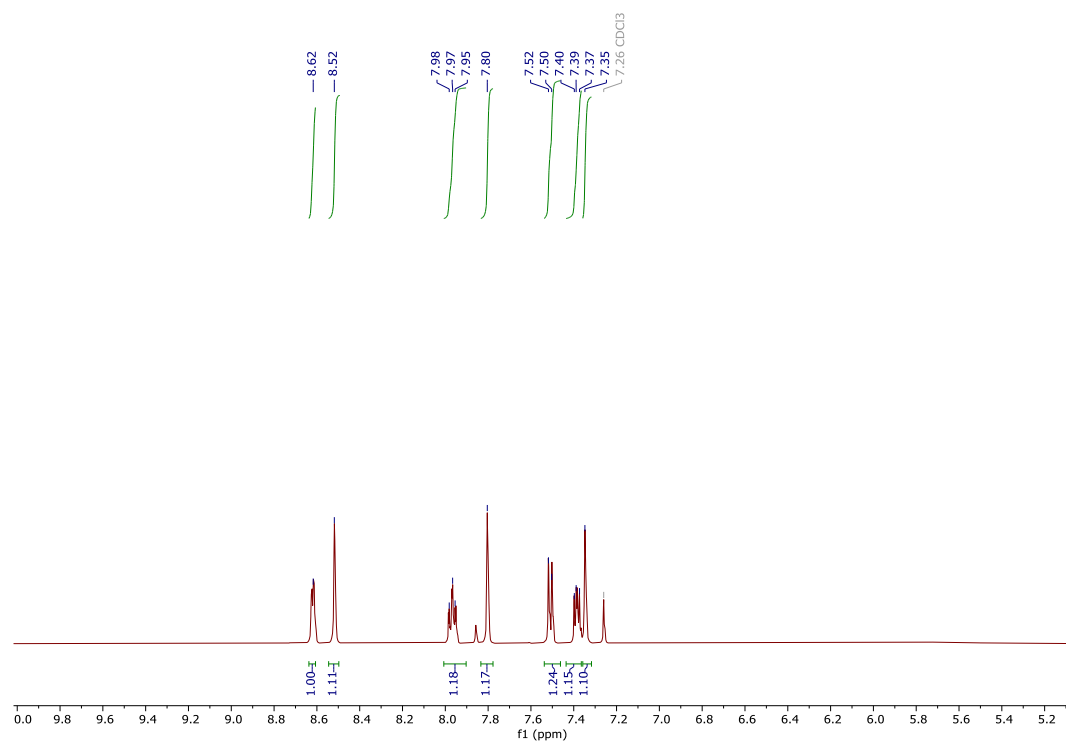


Fig.8: ^1H NMR of Ligand L2

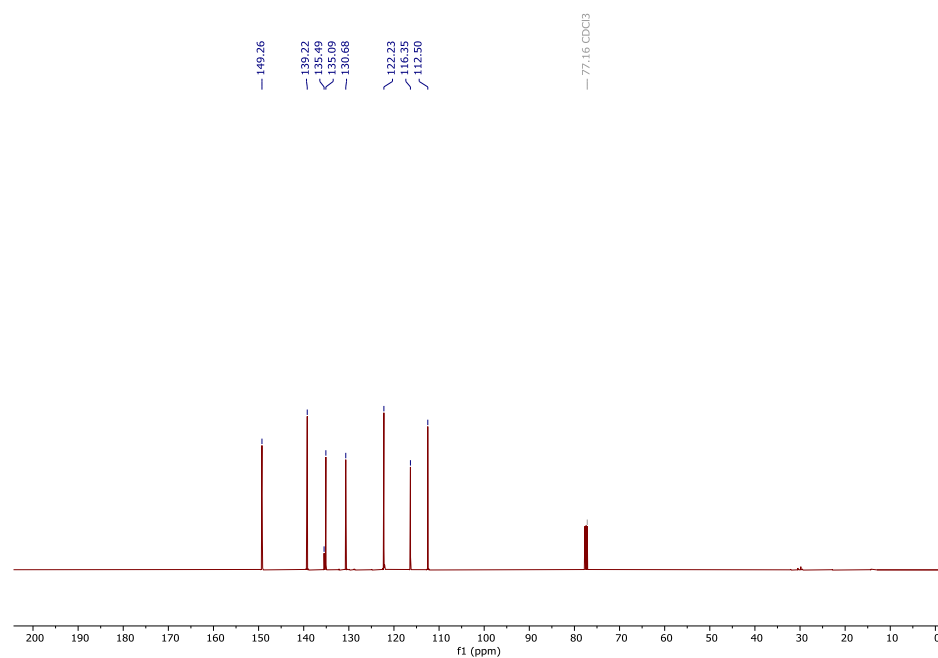


Fig.9: ^{13}C NMR of Ligand L2

3.13 Characterization of Ligand L3

3.13.1 LCMS of Ligand L3

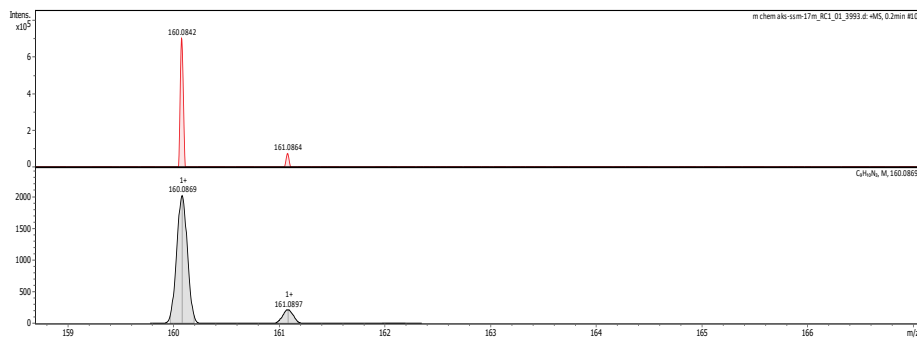


Fig.10: LCMS of Ligand L3

3.13.2 NMR spectra of Ligand L3

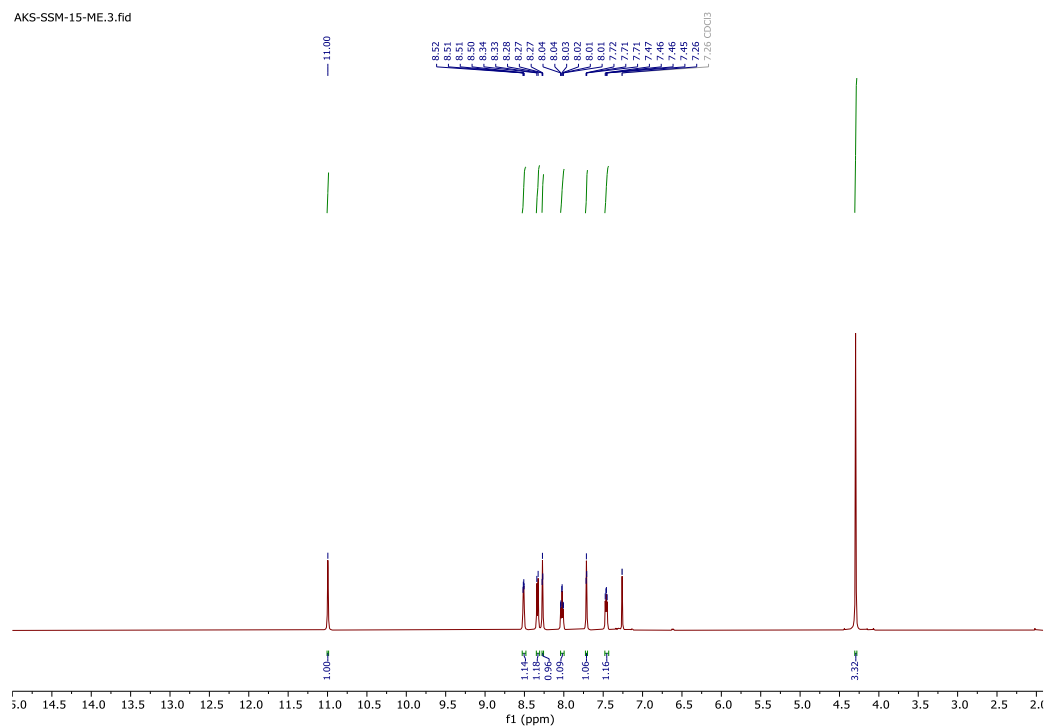


Fig.11: ¹H NMR of Ligand L3

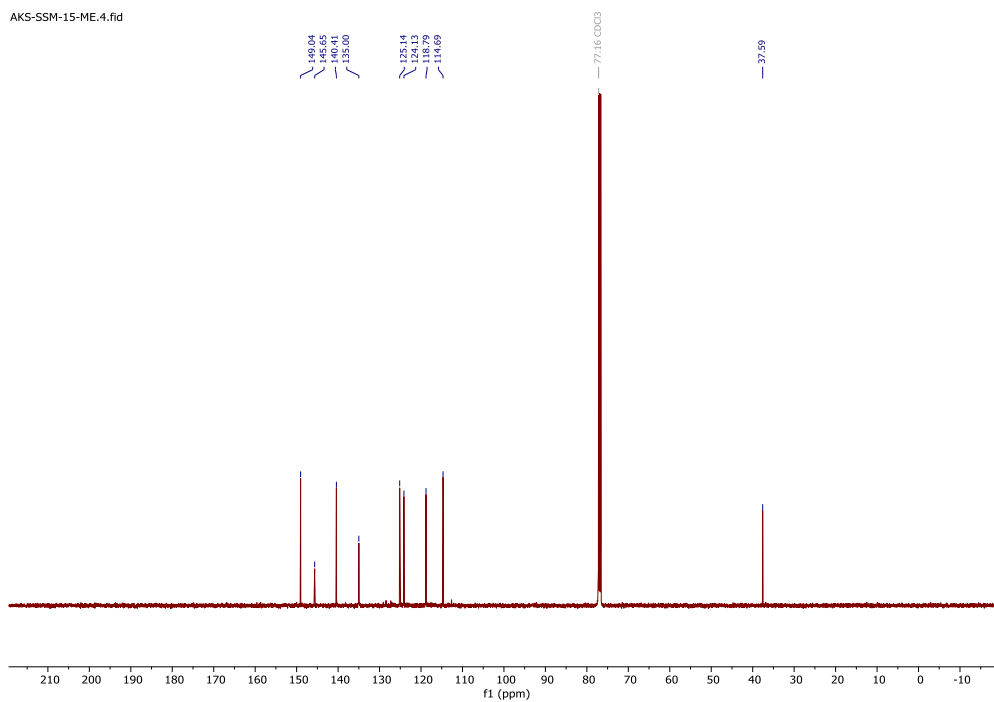


Fig.12: ¹³C NMR of Ligand L3

3.14 Characterization of Ligand L4

3.14.1 NMR spectra of Ligand L4

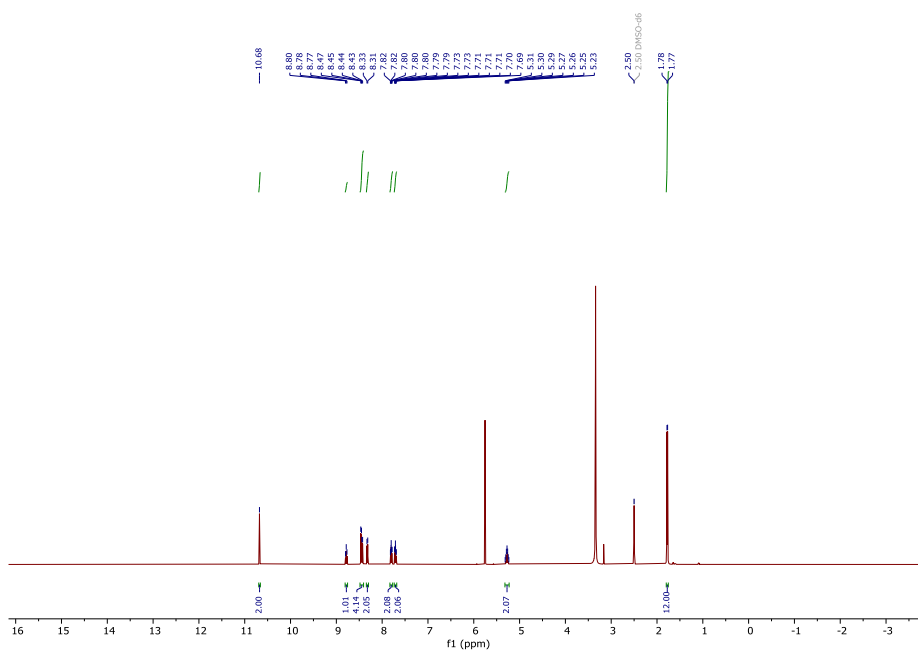


Fig.13: ¹H NMR of Ligand L4

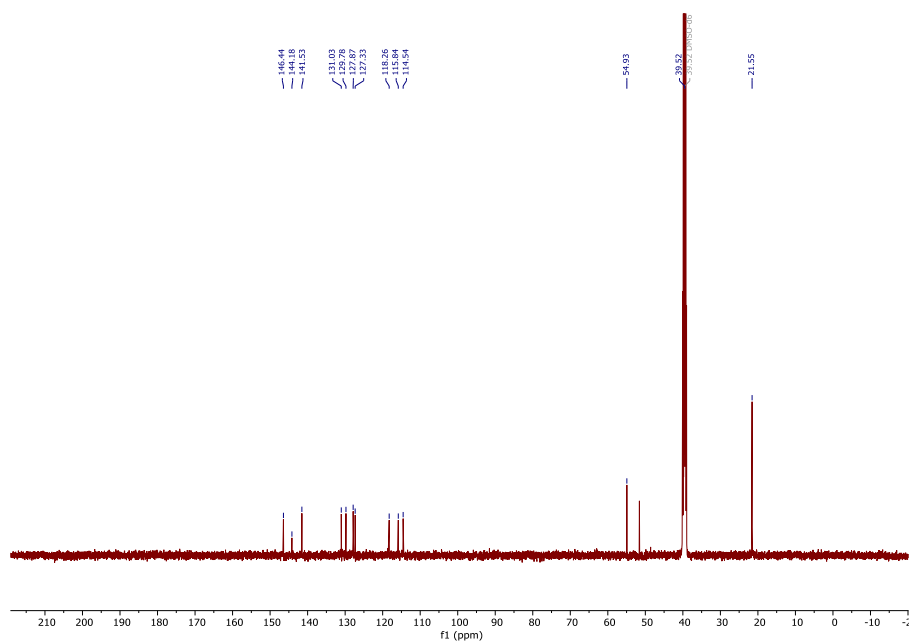


Fig.14: ^{13}C NMR of Ligand L4

3.15 Characterization of Ligand L5

3.15.1 NMR spectra of Ligand L5

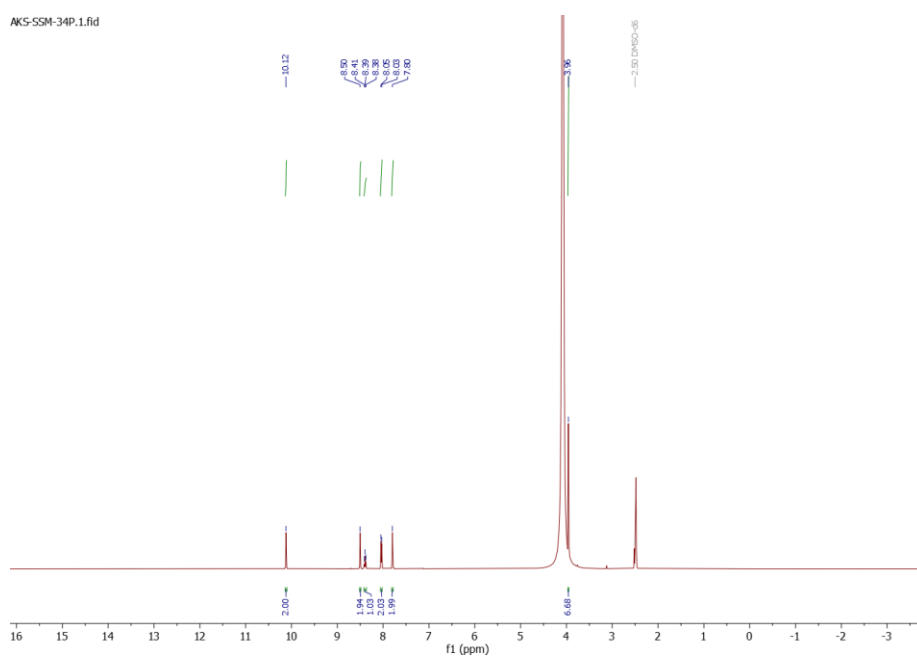


Fig.15: ^1H NMR of Ligand L5

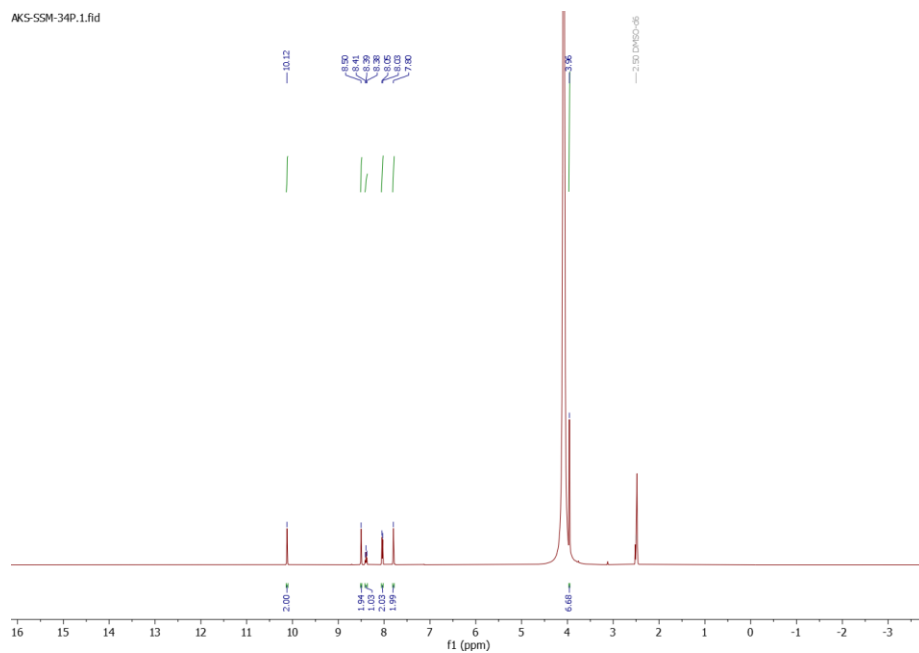


Fig.16: ^{13}C NMR of Ligand **L5**

3.16 Characterization of complex **Ru1**

3.16.1 HRMS of complex **Ru1**

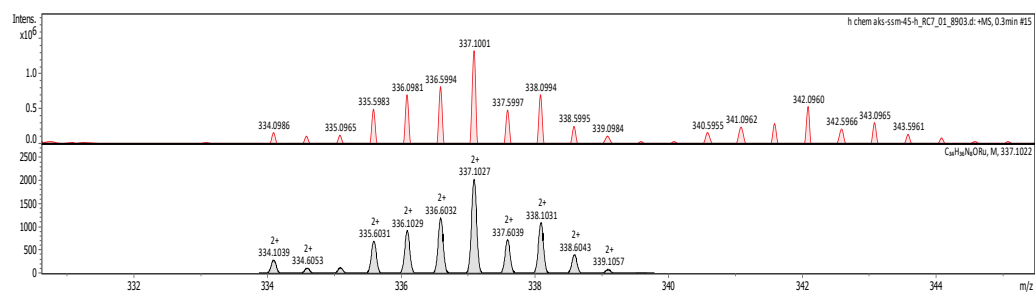


Fig.17: HRMS of complex **Ru1**

3.16.2 NMR spectra of complex **Ru1**

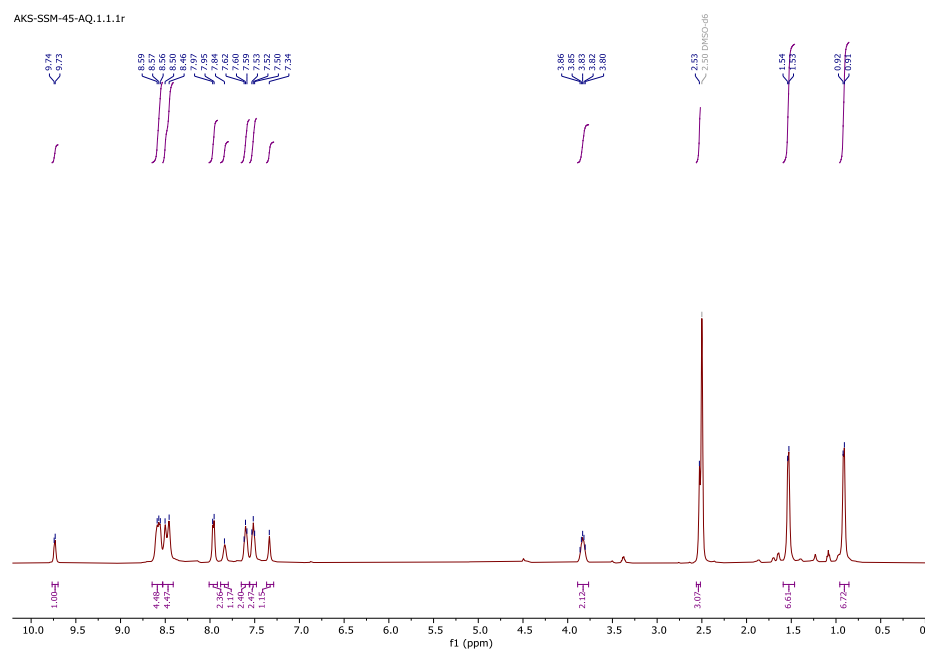


Fig.18: ^1H NMR of Complex **Ru1**

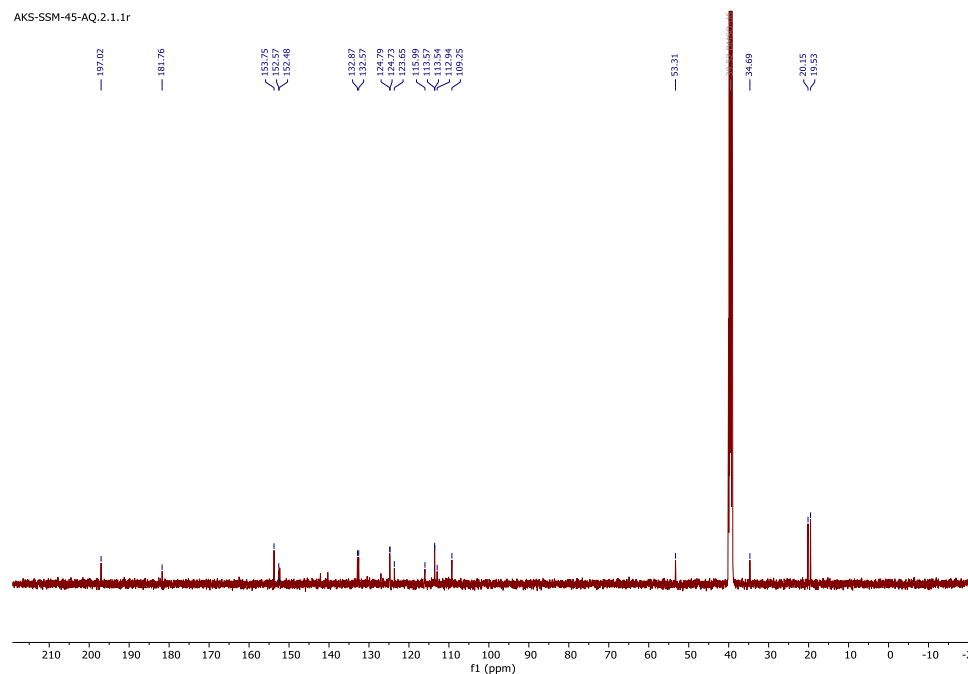


Fig.19: ^{13}C NMR of Complex **Ru1**

AKS-SSM-45-AQ.3.1.1r

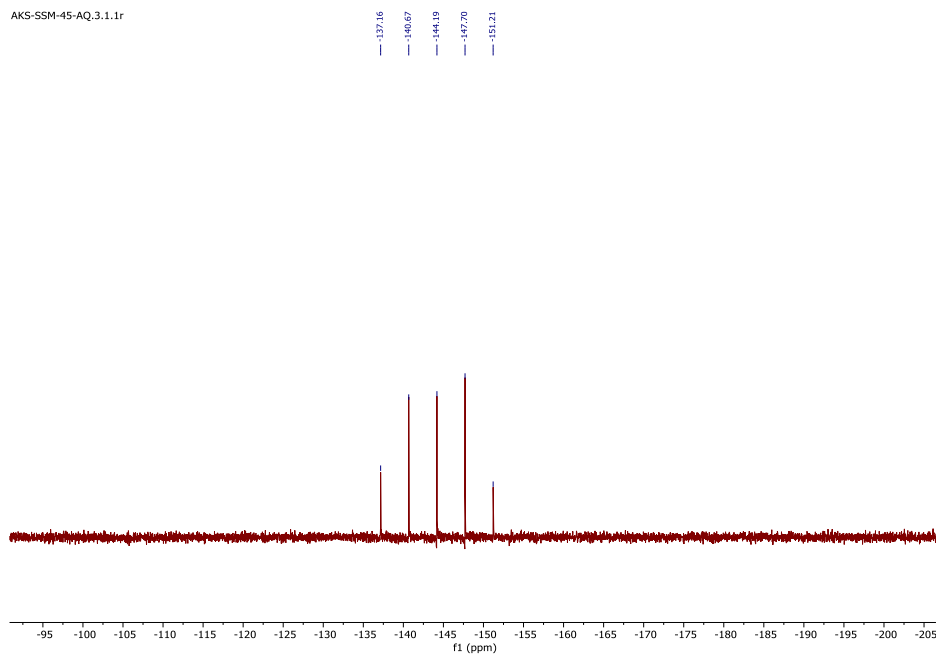


Fig.20: ^{31}P NMR of Complex **Ru1**

AKS-SSM-45-D2.1.1.1r

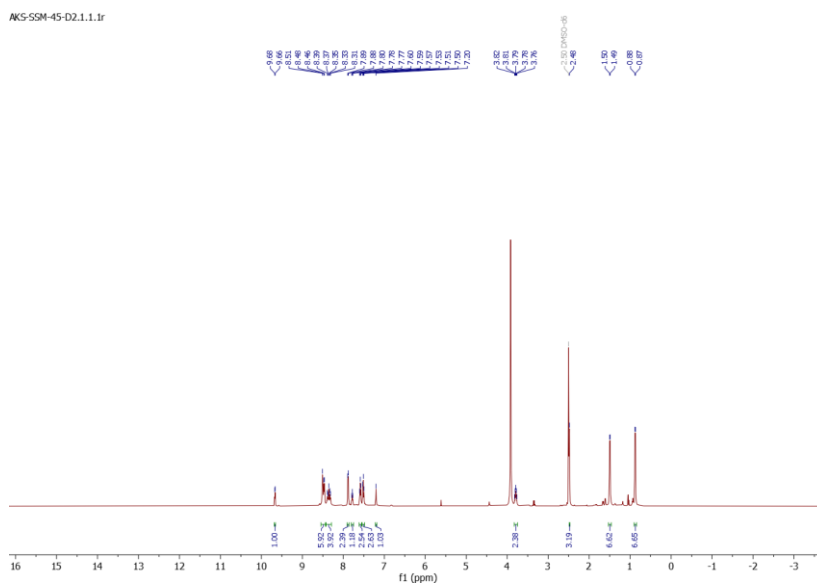


Fig.21: ^1H NMR of complex **Ru1**

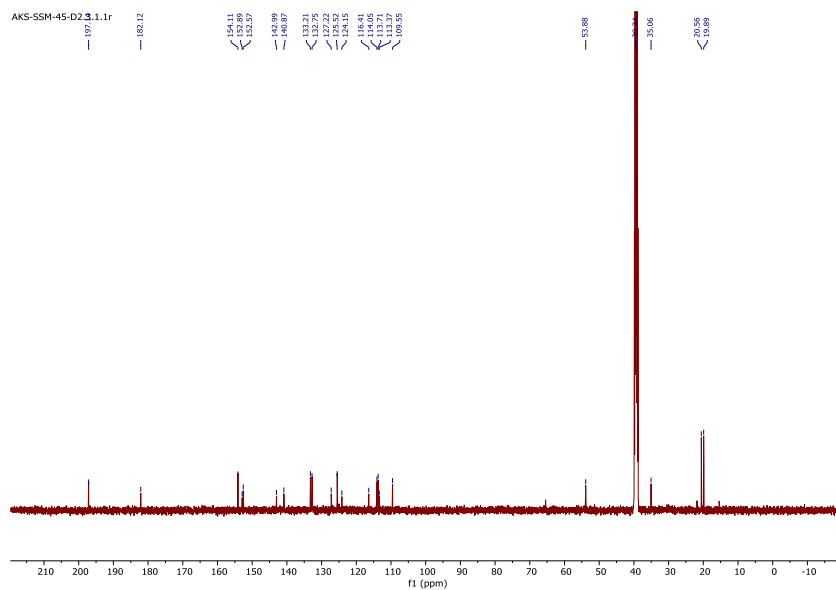


Fig.22: ^{13}C NMR of complex **Ru1**

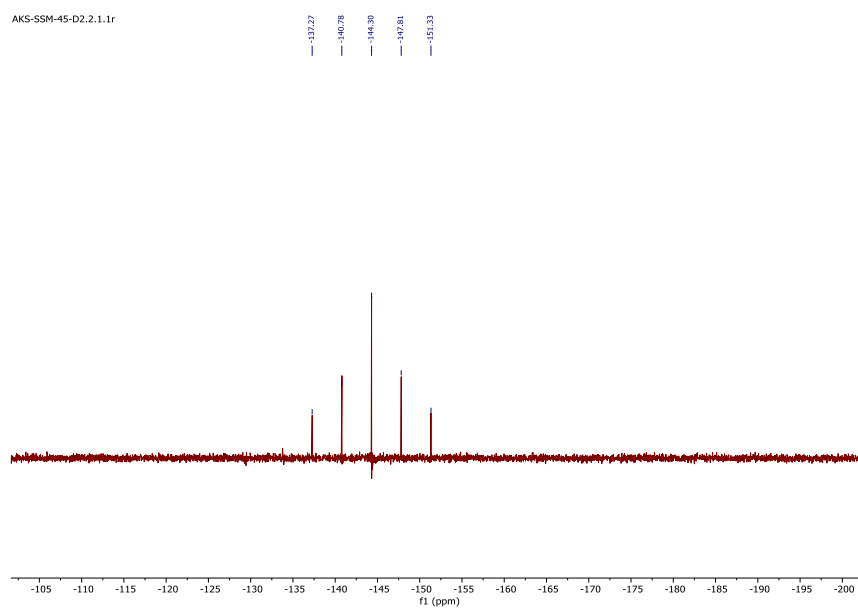


Fig.23: ^{31}P NMR of complex **Ru1**

3.17 Characterization of complex Ru2

3.17.1 LCMS of complex Ru2

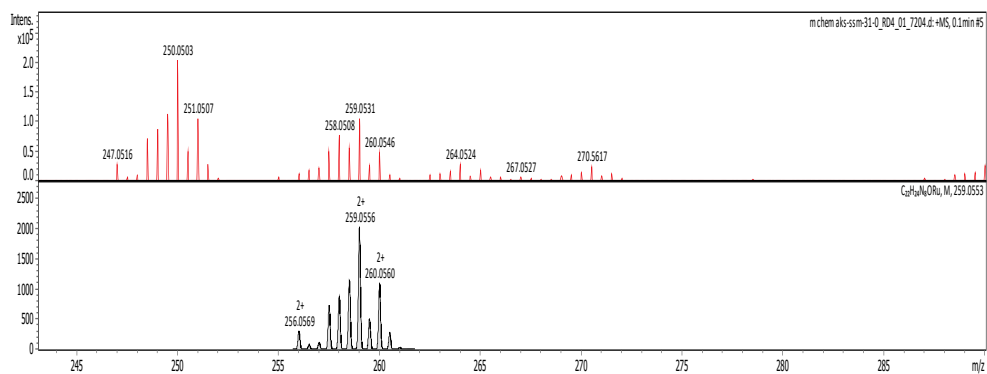


Fig.24: LCMS of complex Ru2

3.17.2 NMR spectra of complex Ru2

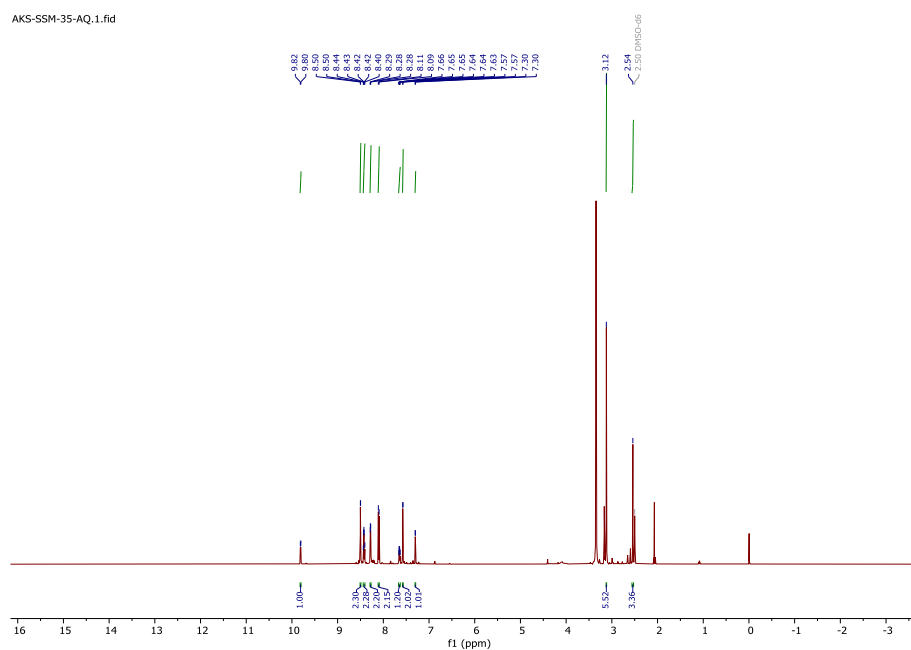


Fig.25: ^1H NMR of complex Ru2

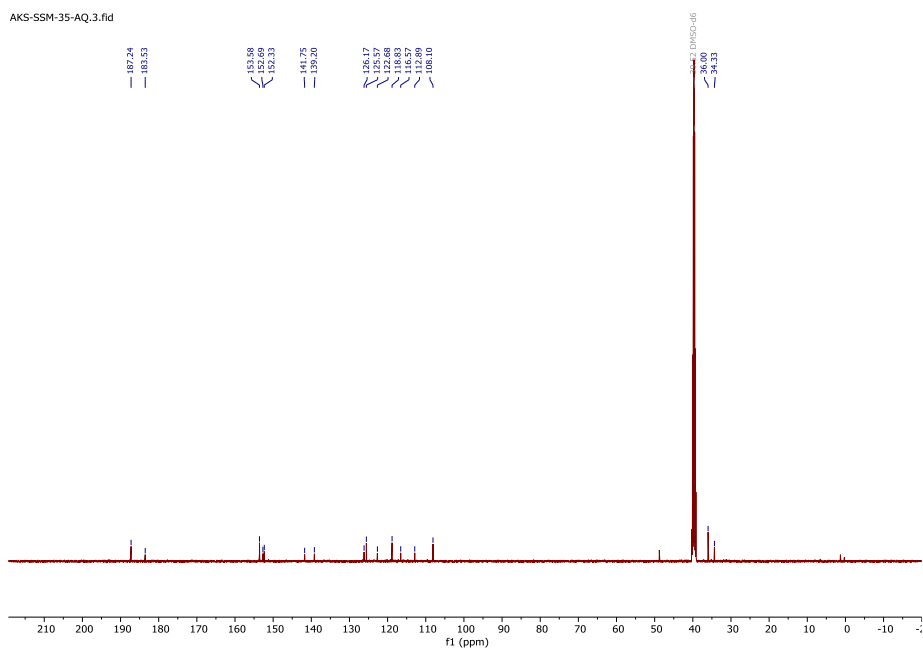


Fig.26: ^{13}C NMR of complex **Ru2**

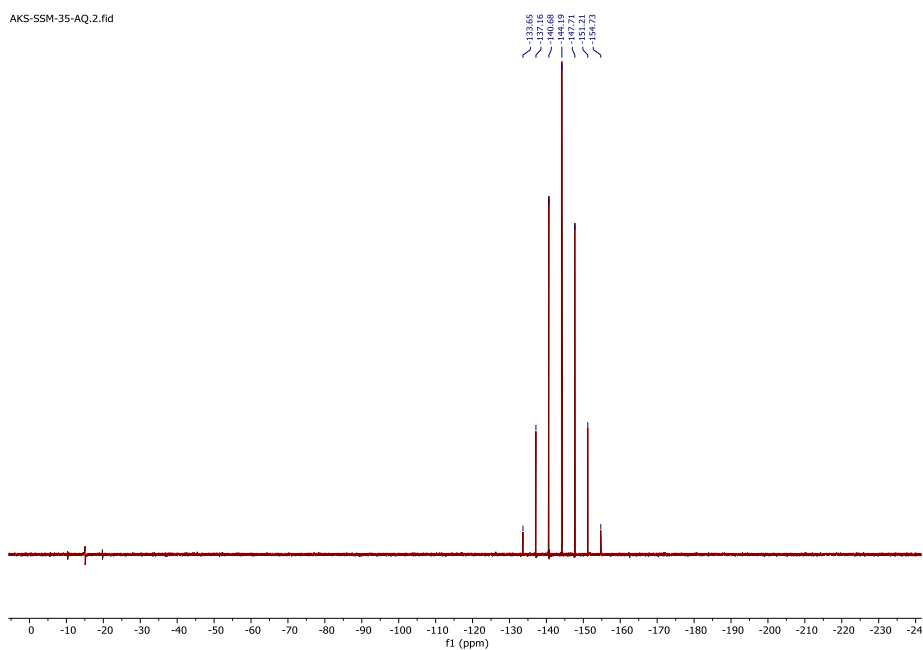


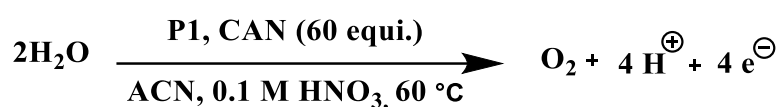
Fig.27: ^{31}P NMR of complex **Ru2**

3.18 CATALYTIC APPLICATIONS:

As a part of our research, we have extensively established the process of water oxidation using **P1**, **P2**, and **Ru1** catalysts including Nitric acid,

perchloric acid, and Triflic acids. However, our findings have revealed that the **Ru1** catalyst was found to have higher catalytic activity in the perchloric acid medium. This discovery emphasizes the pivotal role played by the choice of acid in determining the catalytic performance of the **Ru1** catalyst in water oxidation reactions. As a result, further studies are necessary to uncover the underlying mechanisms that govern this behaviour and optimize the conditions for effectively utilizing the **Ru1** catalyst in the water oxidation reaction.

Oxygen Evolution Experiment in HNO₃:

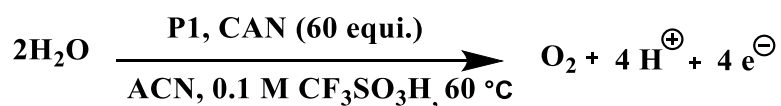


Scheme 11: Oxygen evolution experiment in 0.1M HNO₃

In the experiment, the catalyst Ru2 (5 mg, 0.0053 mol) was dissolved in 2 mL of ACN in an oven-dried 25 mL round-bottom flask. Next, 4 mL of 0.1M HNO₃ mixed with 60 equivalents of CAN (103.34 mg, 0.188 mol) were added to the flask. The reaction mixture was stirred at 60°C until no gas evolution was observed.

Observation: No evolution of gas takes place after 12h.

Oxygen Evolution Experiment in CF₃SO₃H:

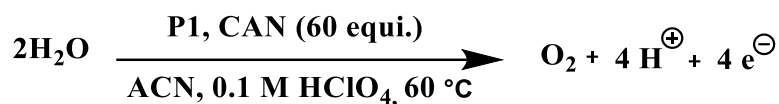


Scheme 12: Oxygen evolution experiment in 0.1 M CF₃SO₃H

In a custom-made 25 mL round bottom flask, CAN was dissolved in 0.1 M CF₃SO₃H while stirring and Nitrogen purging. The catalyst was dissolved in water and added via sidearm. The reaction mixture was stirred and maintained at a temperature of 60°C.

Observation: No evolution of gas takes place after 12h.

Oxygen Evolution Experiment in HClO₄:

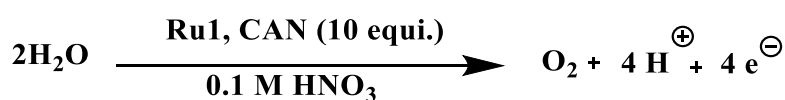


Scheme 13: Oxygen evolution experiment in 0.1 M HClO₄

In a custom-made 25 mL round bottom flask, CAN was dissolved in 0.1 M CF₃SO₃H while stirring and Nitrogen purging. The catalyst was dissolved in water and added via sidearm. The reaction mixture was stirred and maintained at a temperature of 60°C.

Observation: During the experiment, a significant phenomenon was observed involving the evolution of oxygen bubbles over a specific time interval. The initiation of oxygen bubble formation was observed after 10 minutes. Within the subsequent 5 to 6 minutes, a quantified volume of 9 mL of oxygen was evolved. This initial evolution of oxygen bubbles was followed by a steady release of oxygen over the next 20 minutes, resulting in a cumulative release of 14 mL of oxygen. The overall oxygen evolution process continued till the evolution of gas ceased. To ensure the accuracy and consistency of the results, the experiment was repeated twice, and consistent readings were obtained.

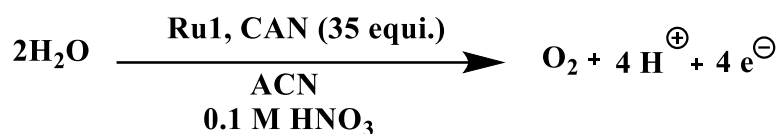
Oxygen Evolution Experiment in HNO₃:



Scheme 14: Oxygen evolution experiment in 0.1M HNO₃.

To experiment, the CAN was dissolved in 0.1 M HNO₃ by stirring and purging with N₂ in a 25 mL round bottom flask that was custom-made for this purpose. The catalyst was then dissolved in water and added through the sidearm to complete the reaction mixture. The reaction mixture was stirred at room temperature until no gas evolution was observed.

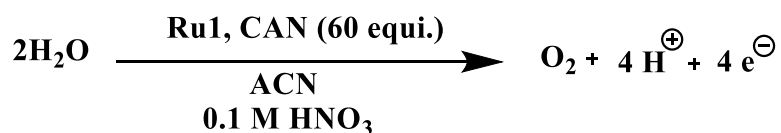
Observation: No evolution of gas takes place after 12h.



Scheme 15: Oxygen evolution experiment in 0.1M HNO₃

A custom-made 25 mL round bottom flask dissolved CAN in 0.1M HNO₃ while stirring and purging with N₂ atmosphere. The catalyst was dissolved in ACN and added via the sidearm. The reaction mixture was stirred and maintained at room temperature.

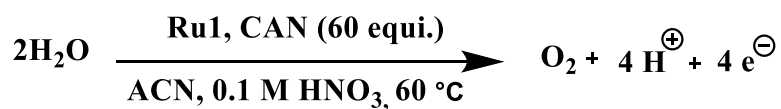
Observation: No evolution of gas takes place after 12h.



Scheme 16: Oxygen evolution experiment in 0.1M HNO₃

In a custom-built 25mL round bottom flask, the catalyst was dissolved in ACN while stirring and Nitrogen purging. CAN was dissolved in 0.1M HNO₃ via the sidearm. The reaction mixture was stirred and maintained at room temperature.

Observation: No evolution of gas takes place after 12h.

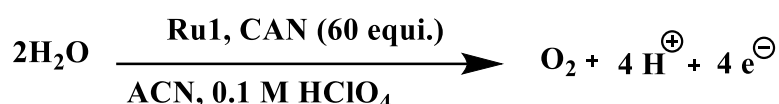


Scheme 17: Oxygen evolution experiment in 0.1M HNO₃

A custom-made 25 mL round bottom flask dissolved CAN in 0.1 M HNO₃ while stirring and purging with N₂. The catalyst was dissolved in ACN and added via the sidearm. The reaction mixture was stirred and maintained at a temperature of up to 60 °C.

Observation: During the experiment, a significant phenomenon was observed wherein the evolution of oxygen bubbles occurred over a specific temporal interval. The onset of oxygen bubble formation was noted 10 minutes post-initiation of the experiment. Within the subsequent 5 to 6 minutes, a quantified volume of 15 mL of oxygen was evolved. This initial evolution of oxygen bubbles was followed by a sustained release of oxygen over the next 15 minutes, resulting in a cumulative release of 27 mL of oxygen. The overall oxygen evolution process continued until the evolution of gas ceased. To ensure the precision and consistency of the results, the experiment was repeated thrice, and consistent readings were obtained

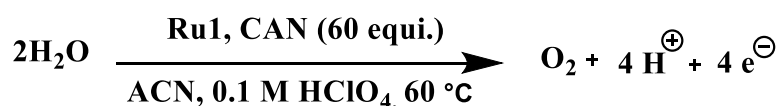
Oxygen Evolution Experiment in HClO₄:



Scheme 18: Oxygen evolution experiment in 0.1M HClO₄

A custom-made 25 mL round bottom flask dissolved CAN in 0.1M HNO₃ while stirring and purging with N₂ atmosphere. The catalyst was dissolved in ACN and added via the sidearm. The reaction mixture was stirred and maintained at room temperature.

Observation: No evolution of gas takes place after 12h.



Scheme 19: Oxygen evolution experiment in 0.1M HClO₄

Observation: During the experiment, a significant phenomenon was observed wherein the evolution of oxygen bubbles occurred over a specific temporal interval. The onset of oxygen bubble formation was noted 10 minutes post-initiation of the experiment. Within the subsequent 5 to 6 minutes, a quantified volume of 15 mL of oxygen was

evolved. This initial evolution of oxygen bubbles was followed by a sustained release of oxygen over the next 15 minutes, resulting in a cumulative release of 27 mL of oxygen. The overall oxygen evolution process continued until the evolution of gas ceased. To ensure the precision and consistency of the results, the experiment was repeated thrice, and consistent readings were obtained.

CHAPTER-4

CONCLUSION:

To summarize, the complex **P1** and **P2** have already been synthesized and characterized in our lab through various spectroscopic techniques, and the complex **Ru1** and **Ru2** were synthesized by me. However, the catalyst **Ru1** is found to have more catalytic activity as compared to others, while the catalyst **P2** showed no catalytic activity in any other acidic medium. It is essential to conduct further studies to gain a complete understanding of catalyst **Ru1**'s catalytic properties and its potential for practical applications in water oxidation catalysis. Ongoing research in this area will help to determine the feasibility and effectiveness of catalyst **Ru1**.

REFERENCES:

1. Singh, R.K., Yadav, D. and Singh, A.K., **2023**. Cationic ruthenium (II)-CNC pincer complexes as phosphine-free catalysts for nitrile hydration to amides in aqueous medium. *Molecular Catalysis*, 549, p.113523.
2. Shahid, N., Singh, R.K., Srivastava, N. and Singh, A.K., **2023**. Base-free synthesis of benchtop stable Ru (iii)-NHC complexes from RuCl₃·3H₂O and their use as precursors for Ru (ii)-NHC complexes. *Dalton Transactions*, 52(13), pp.4176-4185.
3. Amthor, S., Hernández-Castillo, D., Maryasin, B., Seeber, P., Mengerle, A.K., Gräfe, S., González, L. and Rau, S., **2021**. Strong Ligand Stabilization Based on π -Extension in a Series of Ruthenium Terpyridine Water Oxidation Catalysts. *Chemistry—A European Journal*, 27(68), pp.16871-16878.
4. Patel, J., Majee, K., Ahmad, E., Das, B. and Padhi, S.K., **2017**. Effect of pyridyl substitution on chemical and photochemical water oxidation by [Ru (terpyridine)(bipyridine)(OH₂)]²⁺ scaffolds. *European Journal of Inorganic Chemistry*, 2017(1), pp.160-171.
5. Younus, H.A., Su, W., Ahmad, N., Chen, S. and Verpoort, F., **2015**. Ruthenium pincer complexes: synthesis and catalytic applications. *Advanced Synthesis & Catalysis*, 357(2-3), pp.283-330.
6. Soleilhavoup, M. and Bertrand, G., **2015**. Cyclic (alkyl)(amino) carbenes (CAACs): stable carbenes on the rise. *Accounts of chemical research*, 48(2), pp.256-266.
7. Yadav, D., Misra, S., Kumar, D., Singh, S. and Singh, A.K., **2021**. Cationic ruthenium (II)-NHC pincer complexes: Synthesis, characterization and catalytic activity for transfer hydrogenation of ketones. *Applied Organometallic Chemistry*, 35(8), p.e6287.

8. Younus, H.A., Ahmad, N., Su, W. and Verpoort, F., **2014**. Ruthenium pincer complexes: Ligand design and complex synthesis. *Coordination Chemistry Reviews*, 276, pp.112-152.
9. Matheu, R., Ertem, M.Z., Gimbert-Suriñach, C., Sala, X. and Llobet, A., **2019**. Seven coordinated molecular ruthenium–water oxidation catalysts: a coordination chemistry journey: focus review. *Chemical reviews*, 119(6), pp.3453-3471.
10. Koy, M., Bellotti, P., Das, M. and Glorius, F., **2021**. N-Heterocyclic carbenes as tunable ligands for catalytic metal surfaces. *Nature Catalysis*, 4(5), pp.352-363.
11. Öfele, K., 1968. 1, 3-Dimethyl-4-imidazolinylliden-(2)-pentacarbonylchrom ein neuer Übergangsmetall-carben-komplex. *Journal of Organometallic Chemistry*, 12(3), pp.P42-P43.
12. Wanzlick, H.W. and Schönherr, H.J., **1968**. Direct synthesis of a mercury salt-carbene complex. *Angewandte Chemie International Edition in English*, 7(2), pp.141-142.
13. Arduengo III, A.J., Harlow, R.L. and Kline, M., **1991**. A stable crystalline carbene. *Journal of the American Chemical society*, 113(1), pp.361-363.
14. Díez-González, S. ed., **2016**. *N-heterocyclic carbenes: from laboratory to curiosities to efficient synthetic tools* (Vol. 27). Royal Society of Chemistry.
15. Hopkinson, M.N., Richter, C., Schedler, M. and Glorius, F., **2014**. An overview of N-heterocyclic carbenes. *Nature*, 510(7506), pp.485-496.
16. Kundu, A., Barman, S.K. and Mandal, S., **2022**. Dangling Carboxylic Group That Participates in O–O Bond Formation Reaction to Promote Water Oxidation Catalyzed by a Ruthenium Complex: Experimental Evidence of an Oxide Relay Pathway. *Inorganic Chemistry*, 61(3), pp.1426-1437.

17. Shatskiy, A., Bardin, A.A., Oschmann, M., Matheu, R., Benet-Buchholz, J., Eriksson, L., Kärkäs, M.D., Johnston, E.V., Gimbert-Suriñach, C., Llobet, A. and Åkermark, B., **2019**. Electrochemically driven water oxidation by a highly active ruthenium-based catalyst. *ChemSusChem*, *12*(10), pp.2251-2262.
18. Deng, X. and Tüysüz, H., **2014**. Cobalt-oxide-based materials as water oxidation catalyst: recent progress and challenges. *ACS catalysis*, *4*(10), pp.3701-3714.
19. Thomsen, J.M., Huang, D.L., Crabtree, R.H. and Brudvig, G.W., **2015**. Iridium-based complexes for water oxidation. *Dalton Transactions*, *44*(28), pp.12452-12472.
20. Yagi, M. and Kaneko, M., **2001**. Molecular catalysts for water oxidation. *Chemical Reviews*, *101*(1), pp.21-36.
21. Yang, J., An, J., Tong, L., Long, B., Fan, T. and Duan, L., **2019**. Sulfur coordination effects on the stability and activity of a ruthenium-based water oxidation catalyst. *Inorganic Chemistry*, *58*(5), pp.3137-3144.
22. Gersten, S.W., Samuels, G.J. and Meyer, T.J., **1982**. Catalytic oxidation of water by an oxo-bridged ruthenium dimer. *Journal of the American Chemical Society*, *104*(14), pp.4029-4030.
23. Zong, R. and Thummel, R.P., **2005**. A new family of Ru complexes for water oxidation. *Journal of the American Chemical Society*, *127*(37), pp.12802-12803.
24. Zhan, S., De Gracia Triviño, J.A. and Ahlquist, M.S., **2019**. The carboxylate ligand as an oxide relay in catalytic water oxidation. *Journal of the American Chemical Society*, *141*(26), pp.10247-10252.
25. Duan, L., Bozoglian, F., Mandal, S., Stewart, B., Privalov, T., Llobet, A. and Sun, L., **2012**. A molecular ruthenium catalyst with

water-oxidation activity comparable to that of photosystem II. *Nature chemistry*, 4(5), pp.418-423.